Centro Euro-Mediterraneo sui Cambiamenti Climatici

Research Papers
Issue RP0250
November 2014

SERC - Climate Services Division

East China Sea model implementation to simulate coupled mesoscale and tidal dynamics

By **Yu Zhang**
SERC - Climate Services Division, Centro Euro-Mediterraneo sui Cambiamenti Climatici (CMCC)
zhangyu7305@gmail.com

Wang Dong
SERC - Climate Services Division, Centro Euro-Mediterraneo sui Cambiamenti Climatici (CMCC)
dong.wang@cmcc.it

and **Nadia Pinardi**
ANS - Numerical Applications and Scenarios Division, Centro Euro-Mediterraneo sui Cambiamenti Climatici (CMCC)
nadia.pinardi@cmcc.it

and **Paolo Oddo**
ANS - Numerical Applications and Scenarios Division, Centro Euro-Mediterraneo sui Cambiamenti Climatici (CMCC)
paolo.oddo@bo.ingv.it

SUMMARY In this research paper, we will introduce our effect on implantation NEMO in East China Sea with coupled mesoscale and tidal dynamics. First, we detail the model configuration; include the basic physics set, numerical parameters set, and initial and boundary data. Then, we set a series of pseudo barotropic tide numerical experiments, lateral turbulent tracer and momentum diffusion sensitivity experiments and tide dynamic sensitivity experiments. Preliminary conclusions are: The z-partial NEMO need further improvement for reproduce shallow sea tide in complex bathymetry, and s-sigma NEMO better on it. Bilaplacian diffusion scheme can get better Kuroshio strength than laplacian. Tide will produce internal like wave and further affect eddy dynamics. Finally, we summarize our research and bring next plan.

Keywords: NEMO, eddy, tide, kuroshio, numerical sensitive experiment

The work here presented is a part of "Italy-China cooperation: operational oceanography and climate change in coastal and plant seas" We thank Wang Zhaoyi of SERC, who provided the tidal observation harmonic constant of M2 and K1

1. INTRODUCTION

The East China Sea (ECS) is a marginal sea east of china. It is a part of the Pacific Ocean and covers an area of roughly $7.0X10^{10}m^2$, average depth of 1 kilometer with a maximum about 2700 m near westbound of Okinawa Trough. ECS is an extremely dynamic oceanic region, which is influenced by the South China Sea water passing through the Taiwan Strait, the Yellow Seawater by the China Coast Current, the Changjiang River, one of the biggest rivers in the world, Kuroshio and tide.

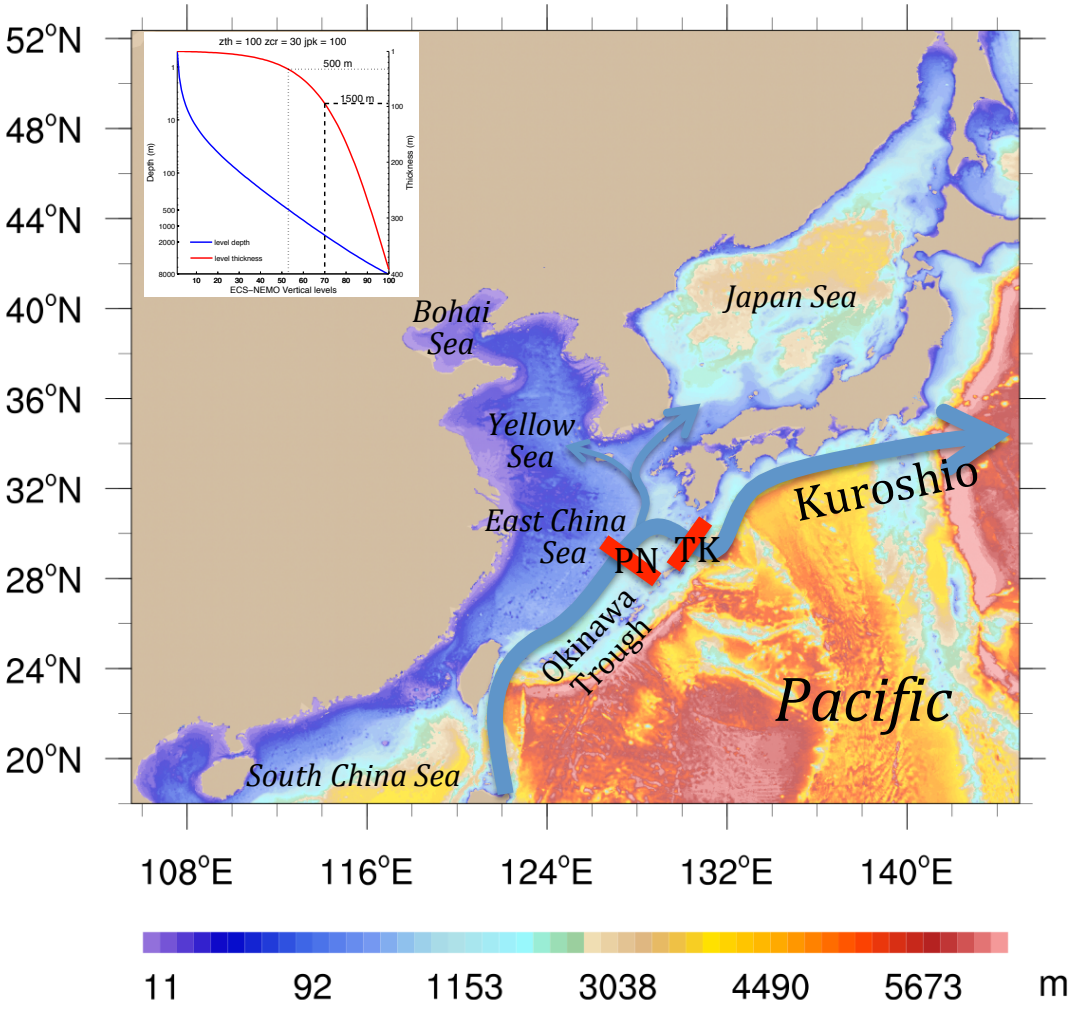

Fig. 1: The geography of East China Sea

The main plot is ECS geography, also for the ECS-NEMO model domain, the red line in figure indicate the famous observation section PN and TK respectively, the blue line represent general conception of Kuroshio and its branches, one flow into China sea and another flow into Japan Sea. The corner plot at left top of main map is ECS-NEMO model vertical levels distribution. Blue line represent level depth and red line represent level thickness, the dotted line marked with 500 m represent the vertical position of 500 m depth in model near level 52, corresponding thickness is 30 m, the similar meaning for 1500 m.

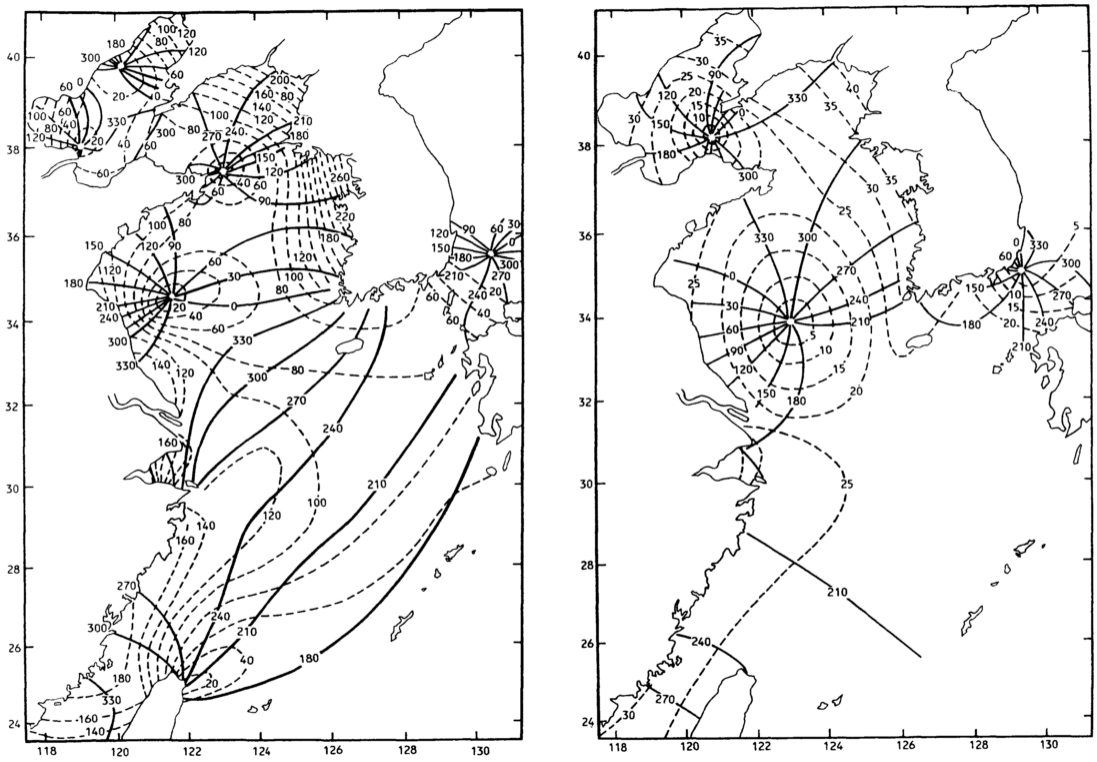

Fig. 2: Co-tidal chart of M2 (left) and K1 (right) from [1]
Solid line is tide amplitude in cm, dotted line is phase lag in degree and referred to 120°E

The kuroshio, which is the western boundary current in the North Pacific, begins off the east coast of Taiwan and flows northeast ward past Japan (as shown in Fig.1 widest blue belt). It can enter the ECS through East Taiwan Channel and Yonaguni-jima Island, then the mainstream of it runs stably along the 200 m isobath in the ECS until approaches the shoaling northern end of the Okinawa Trough, where it separates from the shelf and blends east-southeast ward and eventually flows into the Pacific Ocean through the Tokara Strait. The kuroshio is a warm and salt current, about 100 km wide, and carries a large amount of heat from low to middle latitudes, keeping the climate mild there. It influences not only global ocean climate variations but also the regional ocean system such as ECS.

Tide and tidal current is another one of the most important processes in the ECS, it has been investigated by field observation data, satellite altimetric data and numerical data. As shown in Fig. 2 [1], the distribution of M2 and K1 are rather simple. The maximum M2 amplitude can reach 2.5 m in Hangzhou Bay; it is one of the largest values along the China coast. Taiwan strait is another large M2 amplitude region. There are four M2 amphidromic points, two in Bohai Sea and two in Yellow Sea. K1 amplitude is relatively small in most of China sea, but large in Beibu Gulf (Fig. 3). One of two K1 amphidromic points locate in east of Bohai Sea and another locate in south Yellow Sea.

Since Kuroshio and Tide is so important for ECS that the capable of reproducing the major characteristics of them is a key point in modeling the ECS ocean circulation and this will be our research focus.

2. MODEL GENERAL CONFIGURATION

The ECS general circulation numerical model is based on The Nucleus for European Modelling of the Ocean (NEMO) [2]. The NEMO domain and physical configuration has adjusted for ECS, herein referred as ECS-NEMO.

As shown in Fig.1, the ECS-NEMO covers whole ECS, Yellow Sea, Bohai Sea, Japan Sea, north part of South China Sea and west part of Pacific. The horizontal resolution of model is 1/36 degree, nearly 3 kilometers. The minimum depth of model is 10 m, and the maximum is 8000 m. There are 100 vertical levels in vertical with uneven grid spaces and z-partial coordinate. Levels' thickness ranging from 1 m at surface and 400 m at deepest bottom (Fig. 1). The major physical set of model is shown in Table 1 and 2. C-GLORS [3] used for model start and boundary, ERA Interim [4] used as model atmospheric force. River runoff data come from [5, 6] and add in model as surface boundary E-P flux, the salinity at river influence basin will fix on WOA13 salinity [7]. All fields were remapped on ECS-NEMO grid by SOSIE, which was originally intended to interpolate geophysical fields onto the ORCA family of tripolar grids used by the NEMO OGCM (ORCA2, ORCA1, ORCA05, ORCA025).

Keys	
key_lim2	Louvain-la-Neuve sea ice model version 2
key_bdy	Unstructured Open Boundary Conditions
key_dynspg_ts	Time splitting free surface algorithm
key_traldf_c3d	latitude, longitude, depth dependent tracer diffusion coefficient
key_dynldf_c3d	latitude, longitude, depth dependent dynamic viscosity coefficient
key_ldfslp	lateral diffusion scheme for tracers and momentum
key_zdfric	Vertical diffusion based on the Richardson number
key_mpp_mpi	Enable mutli processing using MPI
key_asminc	Activates assimilation increment

Table 1: ECS-NEMO physical keys sets

rn_rdt/nn_baro	120s/60, time step for the dynamics and tracers/number of barotropic time step
nn_bfr/rn_bfri2	2/1.0e-3, nonlinear bottom friction/bottom drag coefficient
namtra_adv	advection scheme for tracer: TVD scheme
namdyn_adv	vector form formulation for the momentum advection
namdyn_vor	energy and enstrophy conserving scheme for dynamic algorithm
namtra_ldf	horizontal bilaplacian operator for tracers and momentum: -5.0e8
namsbc	CORE bulk formulation, ERA Interim. runoffs, Dai, 2002, 2009, use woa13 for salinity information of runoff
Lateral boundary	no slip for lateral momentum boundary condition bdy: Flather radiation scheme for the barotropic variables, Flow Relaxation Scheme (FRS) available for others, TSUV data come from C-GLORS, Tide data come from OTPS2

Table 2: ECS-NEMO model parameters sets

3.PSEUDO BAROTROPIC TIDE EXPERIMENTS

First of all, we do a series of pseudo barotropic experiments to check tide reproduce capacity of ECS-NEMO. Temperature and salinity will fix on 10°C and 35 PSU in pseudo barotropic experiments respectively. Atmospheric force, river runoff, lateral boundary of temperature, salinity and baroclinic current will close or fix on zero. We use OTPS2 tide sea level as reference since we don't have observation data. OTPS is an efficient software for predict tide or extract tide harmonic constants from barotropic tidal solutions, it combine TOPX satellite and tidal station observation data assimilation [8]. The M2 and K1 co-tidal chart of OTPS2 at ECS-NEMO region as shown in Fig. 4. One can see that they are quite similar with Fig. 2 and good match with observations (from published articles), especially for amplitude of K1.

Unfortunately, we still struggle in getting a result as good as OTPS. There have some researches such as [9] can obtain numerical tide simulation match observation very well, even their experiments under low space resolution and only use M2 tidal sea level at lateral boundary. However, we can't get good M2 amplitude under similar boundary set. As shown in Fig. 4a1, a2 and a3, a huge difference will appear in M2 amplitude in experiment with tidal level or tidal current at boundary alone, and only with both of them can make ECS-NEMO M2 match OTPS better.

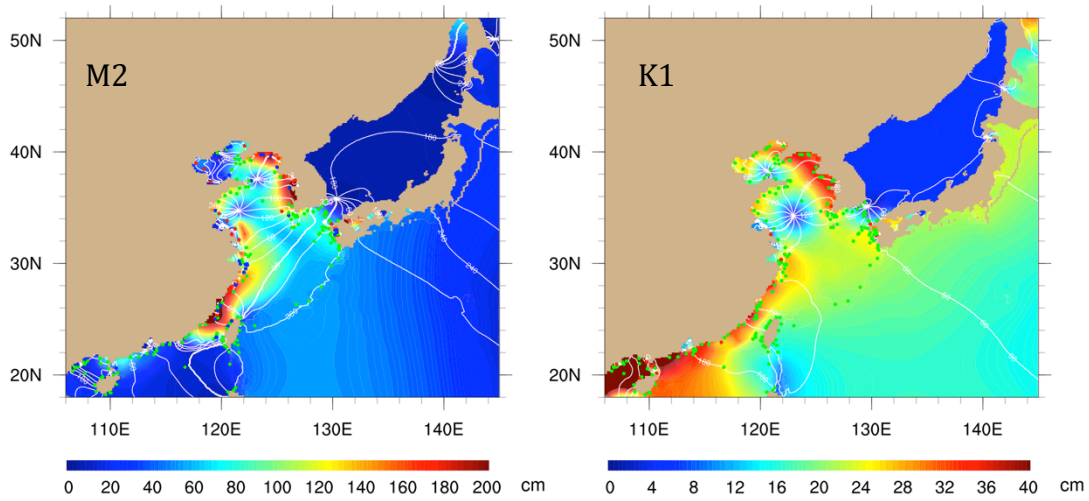

Fig. 3: Co-tidal chart of OTPS2 at ECS-NEMO region
The color shade in figure is tidal harmonic amplitude, and white contour lines are tidal harmonic phase (referred to 0°E). The red filled circles represent amplitude difference between OTPS and observation larger than 30 cm, blue circles mean error larger than 10 cm and less than 30 cm, and green circles mean error less than 10 cm.

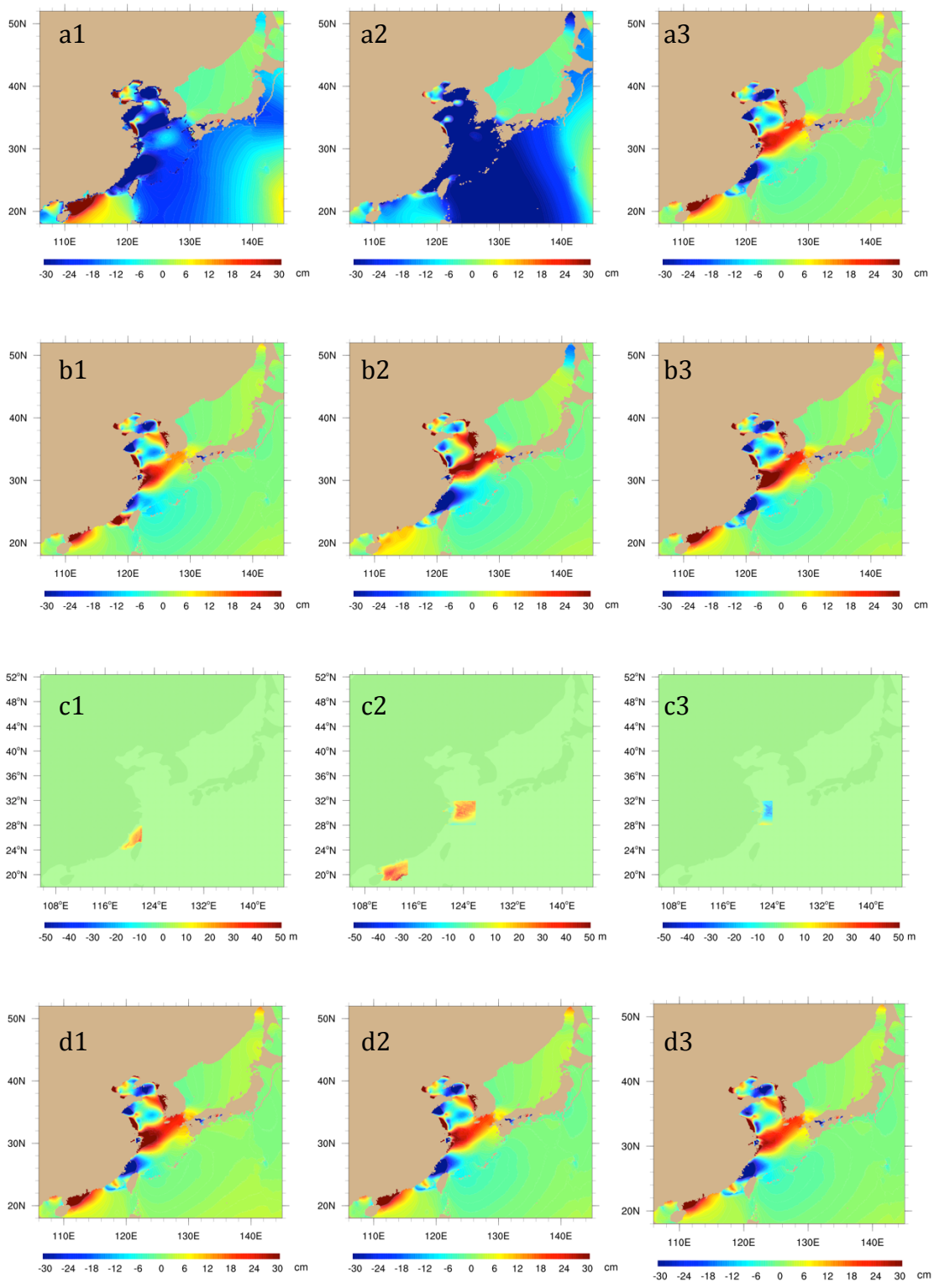
a1
a2
a3
b1
b2
b3
c1
c2
c3
d1
d2
d3
cm
m

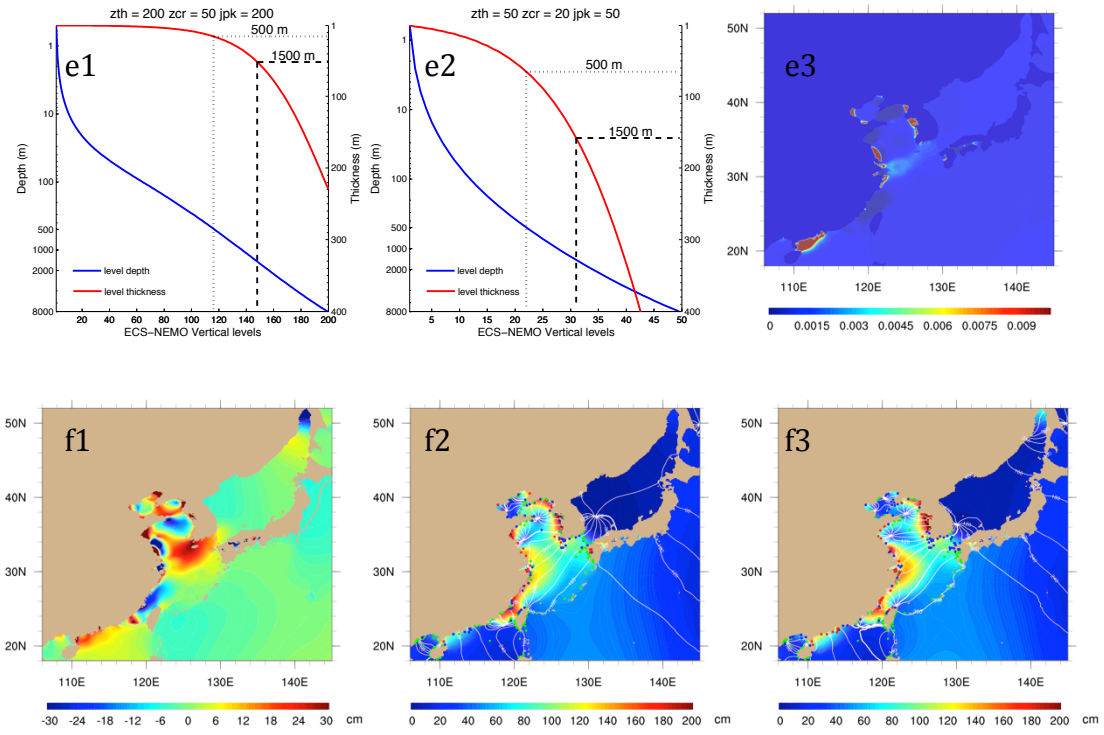

Fig. 4: Co-tidal chart of ECS-NEMO pseudo barotropic tide experiments a1, the difference of M2 amplitude between NEMO-ECS and OTPS with tidal level at boundary alone; a2, same as a1 but for experiment with tidal current at boundary alone; a3, same as a1 but for experiment both with tidal sea level and current at boundary, and a3 will also as our control experiment; b1, same as a3 but under bathy change shown in c1; b2, same as a3 but under bathy change shown in c2; b3, same as a3 but under bathy change shown in c3; c1, bathy meter change after deepen bathy at north of Taiwan strait slightly; c2, bathy meter change after deepen bathy at Changjiang and Pearl River estuary slightly; c3, bathy meter change after shoal bathy at Changjiang estuary slightly; d1, same as a3 but for experiment increase vertical resolution; d2, same as a3 but for experiment decrease vertical resolution; d3, same as a3 but under bottom friction coefficient change shown in e3; e1, vertical level distribution of d1; e2, vertical level distribution of d2; e3, the difference of bottom friction coefficient between d3 and control value, constant $1.0e10^{-3}$ everywhere; f1, same as a3 but for s-sigma vertical coordinate experiment; f2 is M2 co-tidal chart of ECS-NEMO under s-sigma coordinate; f3 same as f2 but for ECS-NEMO under z-partial coordinate.

In order to improve tide simulation, we first research the relationship between water depth and M2 amplitude. As shown in Fig. 4b1, b2, b3, c1, c2 and c3, when we deepen the water at north Taiwan Strait, M2 amplitude will increase in whole strait even include south part, where batymetry no change. But when we do the similar thing at Changjiang and Pearl River estuary, M2 amplitude will decrease huge at the latter and little at the former. However, deepen bathymetry at Changjiang River estuary will also increase M2 amplitude in Yellow

Sea and Bohai Sea largely. And if we shallow water at Changjiang River estuary, M2 amplitude will increase more than 20 cm, but Yellow Sea and Bohai Sea change little. Thus, Taiwan Strait and Pearl River estuary have relatively independent tide system, although bathymetry impact on them contrarily. However, the relationship of tide system and bathymetry near Changjiang River estuary more complicated and need further research.

In general, increase model resolution will improve simulation. But M2 amplitude at Changjiang River estuary even bad (Fig. 4d1) when we increase vertical levels from 100 to 200 (Fig. 4e1). And they are almost no change (Fig. 4d2) compare with Fig. 4a3 when we decrease vertical levels from 100 to 50 (Fig. 4e2). Thus, we think vertical resolution is not key point for improve tide simulation and a relatively low resolution will enough, for z-partial coordinate at least. Bottom friction coefficient's impact on tide simulation also insignificantly as shown in Fig. 4d3 and 4e3. For example, even we ten times coefficient, it still can't reduce M2 amplitude at Pearl River estuary much. However, s-sigma will get a much better tide simulation (Fig. 4f1 and 4f2), especially at Taiwan Strait and Pearl River estuary. The possible reason for this is s-sigma coordinate will have an identic bottom boundary, but z-partial coordinate's bottom level thickness will change largely in different bathymetry, shallow sea bottom thinner than deepen ocean. A new bottom boundary code is preparing for z-partial NEMO, and this work will continue when it ready.

4.LATERAL TURBULENT DIFFUSION AND FRICTION COEFFICIENT SENSITIVITY EXPERIMENT

Lateral turbulent diffusion and friction coefficient is one of the most important parameters in ocean numerical model. Unfortunately, we still can't determine the exactly coefficients for a model. Thus, adjustment this parameter and try to get a best simulation is the only way we can do and many researches also point that change it will huge effect ocean simulation, especially on sea current [10].

There are two kinds of lateral turbulent parameter scheme, one is laplacian and another is bilapacian. Generally, laplacian more suit for low resolution and bilapacian usually used in high resolution. However, we will test both of them in this research.

Barotropic transport across PN and TK section, the location of them can be found in Fig. 1, is the most popular index for measuring the intensity of Kuroshio. And it also represents the strength of ocean current. As shown in Fig. 5, the transport of PN section of ECS-NEMO (Fig. 5b) closer observation (Fig. 5a) compare with reanalysis. ECS-NEMO's transport same with C-GLORS at start, and then it continue reduce and upraise again near final of the year. Although the Sverdrup still larger than observation, the trend with time is quite similar. This may due to the finer resolution of ECS-NEMO. All experiments have similar Sverdrup and laplacian slight smaller than bilaplacian. This result can be found in the transport through TK section (Fig. 5c) too. The difference of transport between PN and TK of ECS-NEMO (Fig. 5e) is about 0 to 8 Sv, this number larger than observation (Fig. 5d) in the same time period, which is about 2 Sv. This means that more seawater enter into China Sea from Kuroshio in our model. The detail dynamics of this phenomenon and its influence need further research.

Beside the transport, the shape of Kuroshio also different between bilaplacian and laplacian experiments. As shown in Fig. 6, Kuroshio is weaker under laplacian (Fig. 6d) than bilapacian (Fig. 6b and 6c). And there should has an eddy at south of Kuroshio near east boundary after 3 month from start, but in

laplacian experiments there have nothing and Kuroshio too wide near east boundary. C-GLORS shows strongest Kuroshio again and more bent than ECS-NEMO at north of Taiwan and less bent at south of Kyushu (Fig. 6a). However, since the bad performance of laplacian experiments, we will abandon it in future discuss.

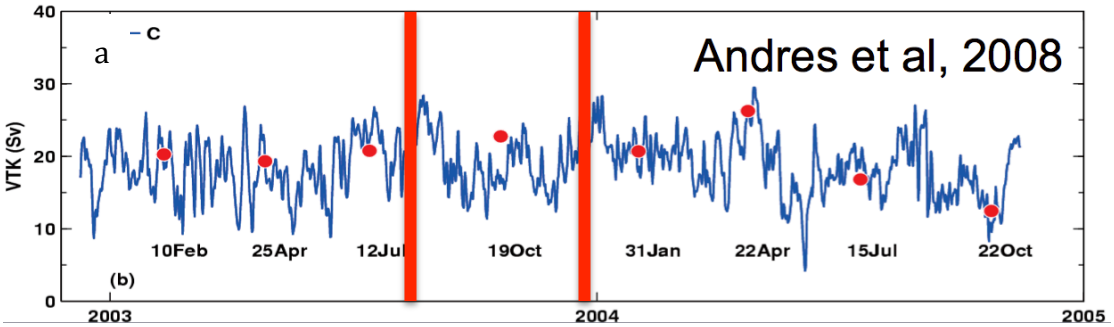

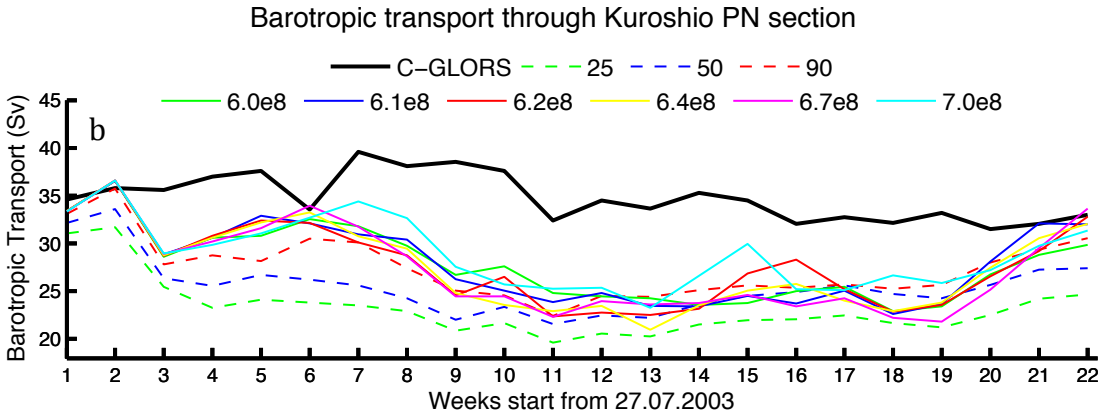

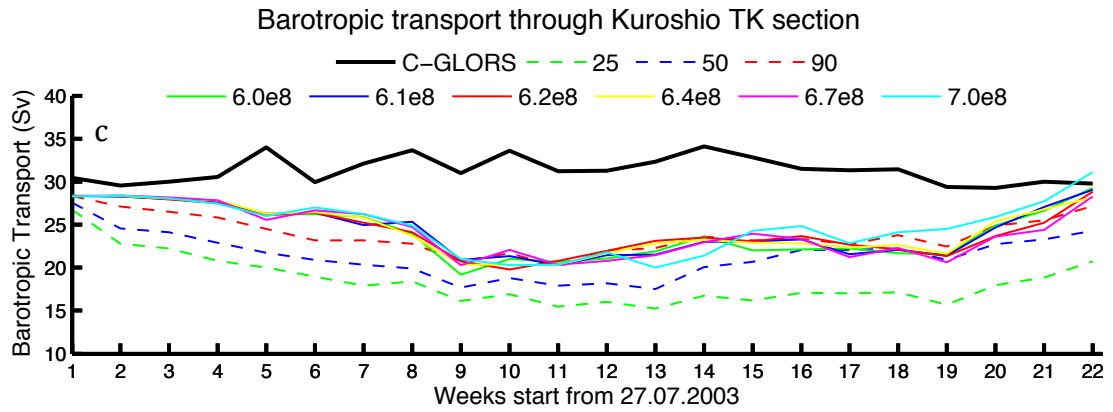

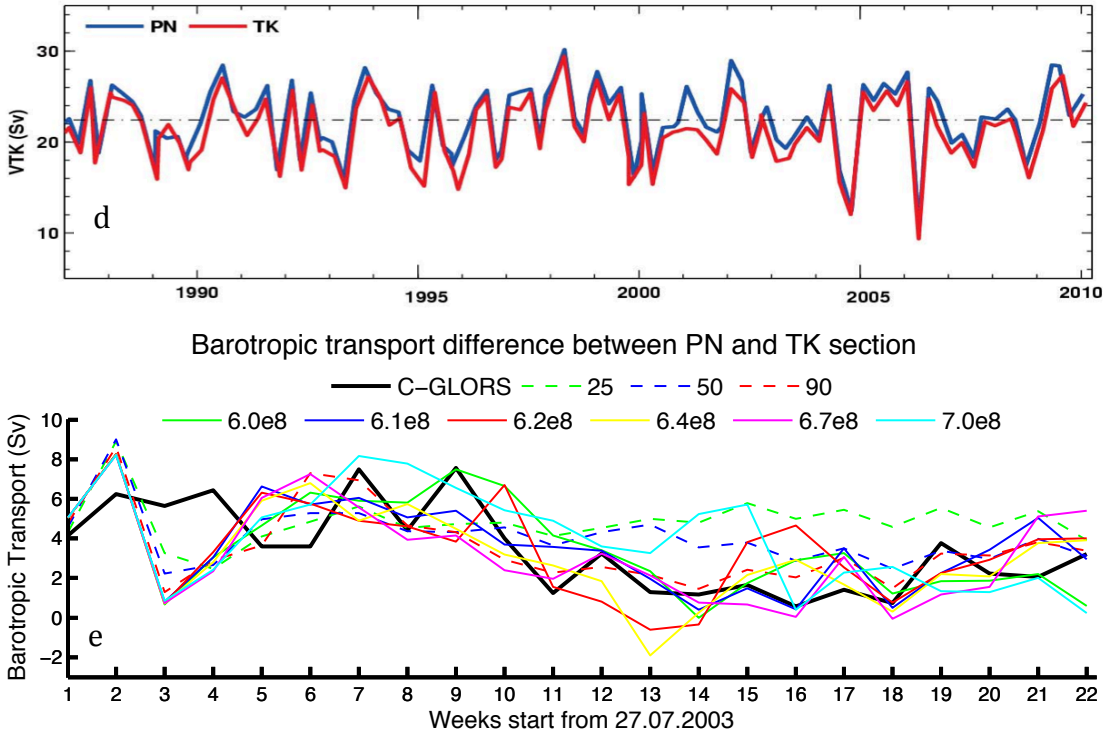

Fig. 5: Barotropic transport across PN and TK section
a is barotropic transport for PN section, it come from [11], the blue line in figure is transport and unit is Sv ($10^6 m^3/s$), the red vertical line indicate ECS-NEMO experiments period; b is barotropic transport of PN section of ECS-NEMO experiments, black line is transport of C-GLORS, color solid lines are transport of ECS-NEMO bilaplacian experiments and the number represent different coefficient we used, color dotted lines same as solid ones but for laplacian experiments; c same as b but for TK section; d same as a but add TK section and for a long time; e same as b but for the difference between TK and PN.

In bilaplacian experiments, we find that even they have similar Kuroshio, the eddy can have remarkable difference. We choose a cold core eddy (the green circle near red arrow in Fig. 7a and 7b) as our research object here, which drop off from Kuroshio Extent and move west slowly and dead in Kuroshio finally (Fig. 7a, 7c and 7d). When bilaplacian coefficient larger than $6.1 \times 10^8 m^4/s$, such as $7.0 \times 10^8 m^4/s$, the eddy will move south slowly and live longer (Fig. 7b). But when the coefficient smaller than $6.0 \times 10^8 m^4/s$, such as $5.0 \times 10^8 m^4/s$, the eddy will move north fleetly and disappear in Kurshio (Fig. 7a). The reason for the eddy has two forward directions is clearly. Because the sea mountain at the eddy bifurcation point, the eddy have to move along the deeper water (Fig. 7e and 7f). These shows that even eddy shallower than sea floor, it still can feel it. However, even we can get the similar move path for the eddy, we can't reproduce the eddy move speed, it always moves faster than reanalysis or observation and this also need further research.

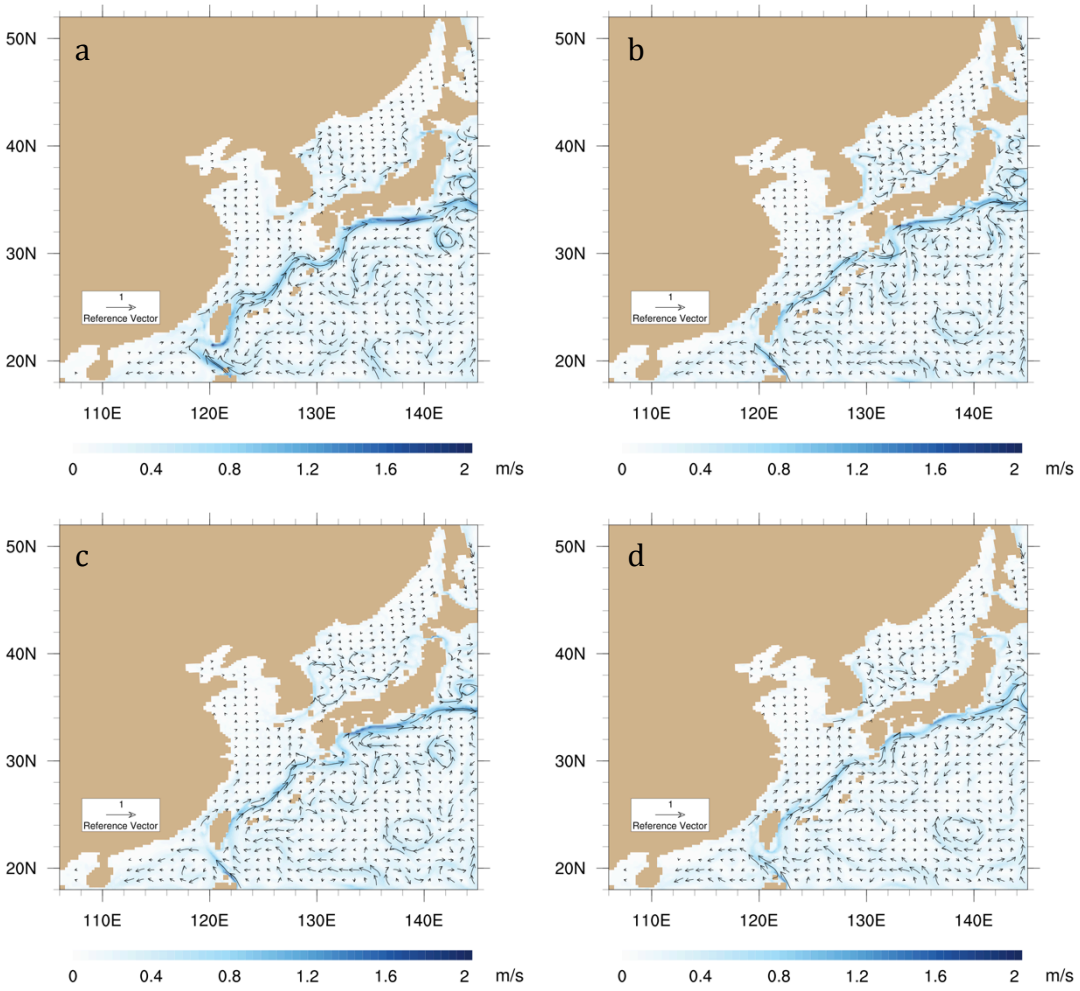

Fig. 6: Sea surface current after 3 month of start
a is C-GLORS data plot, shade in figure is sea surface current speed; b is ECS-NEMO bilaplacian experiment and the coefficient is $5.0 \times 10^8 m^4/s$; c same as b but coefficient is $7.0 \times 10^8 m^4/s$; d is ECS-NEMO laplacian experiment and the coefficient is $50 m^2/s$

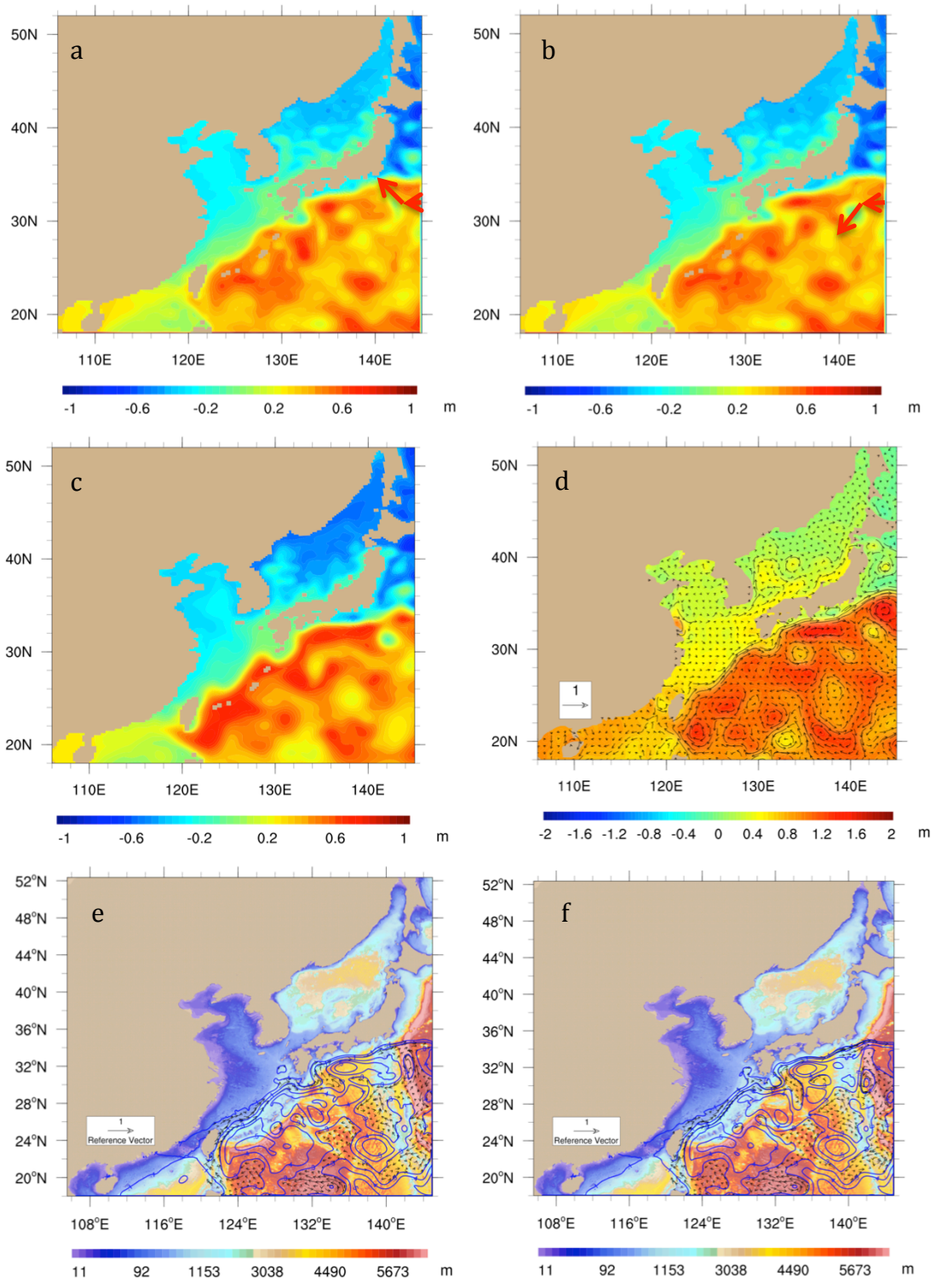
a
50N
40N
30N
20N
110E
120E
130E
140E
-1
-0.6
-0.2
0.2
0.6
1
m
b
50N
40N
30N
20N
110E
120E
130E
140E
-1
-0.6
-0.2
0.2
0.6
1
m
c
50N
40N
30N
20N
110E
120E
130E
140E
-1
-0.6
-0.2
0.2
0.6
1
m
d
50N
40N
30N
20N
1
110E
120E
130E
140E
-2
-1.6
-1.2
-0.8
-0.4
0
0.4
0.8
1.2
1.6
2
m
e
52°N
48°N
44°N
40°N
36°N
32°N
28°N
24°N
20°N
1
Reference Vector
108°E
116°E
124°E
132°E
140°E
11
92
1153
3038
4490
5673
m
f
52°N
48°N
44°N
40°N
36°N
32°N
28°N
24°N
20°N
1
Reference Vector
108°E
116°E
124°E
132°E
140°E
11
92
1153
3038
4490
5673
m

Fig. 7: Sea surface height after 3 month of start
a is ECS-NEMO bilaplacian experiment and the coefficient is $5.0 \times 10^8 m^4/s$, shade in figure is sea surface height, the red arrow indicate move path of eddy; b same as a but coefficient is $7.0 \times 10^8 m^4/s$; c same as a but plot with C-GLORS; d same as a but plot with ARMOR and add velocity vector above it; e same as a but plot SSH (blue contour lines) and velocity vector on color shaded bathymetry; f same as e but coefficient is $7.0 \times 10^8 m^4/s$.

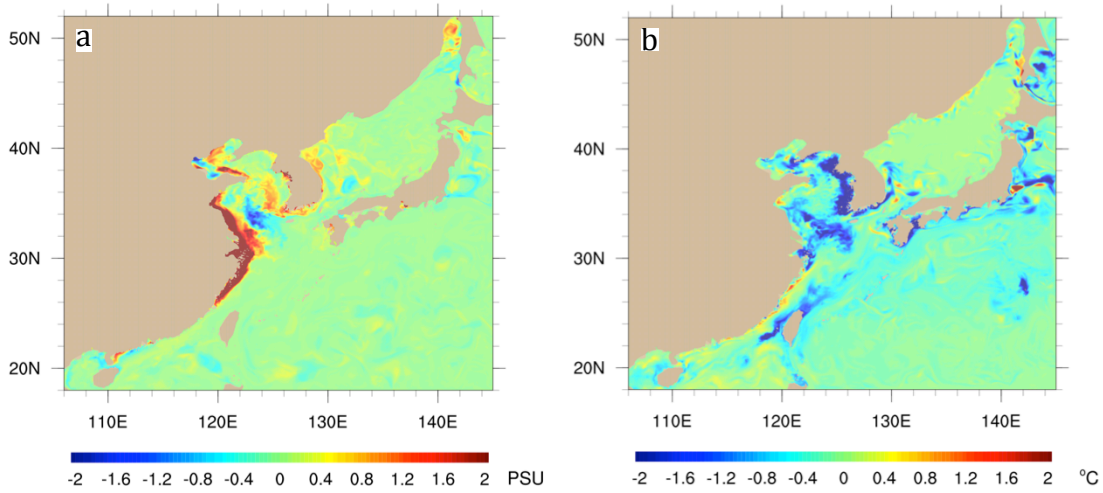

Fig. 8: Tide's effect on shallow sea
a is tide's effect on sea surface salinity after model run 1 month, experiment with tide minus without tide; b is same as a but for sea surface temperature.

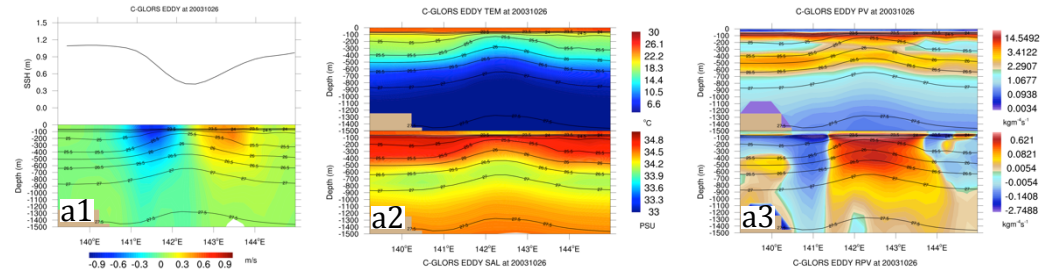
C-GLORS EDDY at 20031026
C-GLORS EDDY TEM at 20031026
C-GLORS EDDY PV at 20031026
a1
a2
a3
C-GLORS EDDY SAL at 20031026
C-GLORS EDDY RPV at 20031026

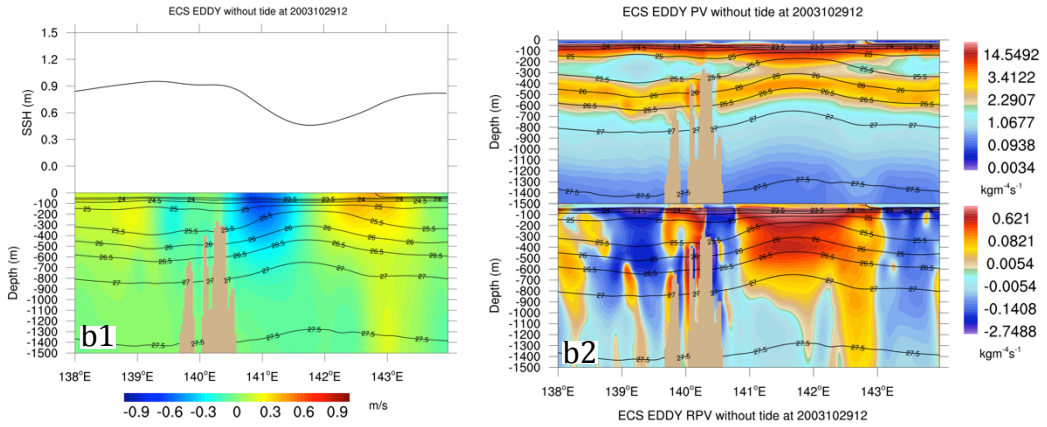
ECS EDDY without tide at 2003102912
ECS EDDY PV without tide at 2003102912
b1
b2
ECS EDDY RPV without tide at 2003102912

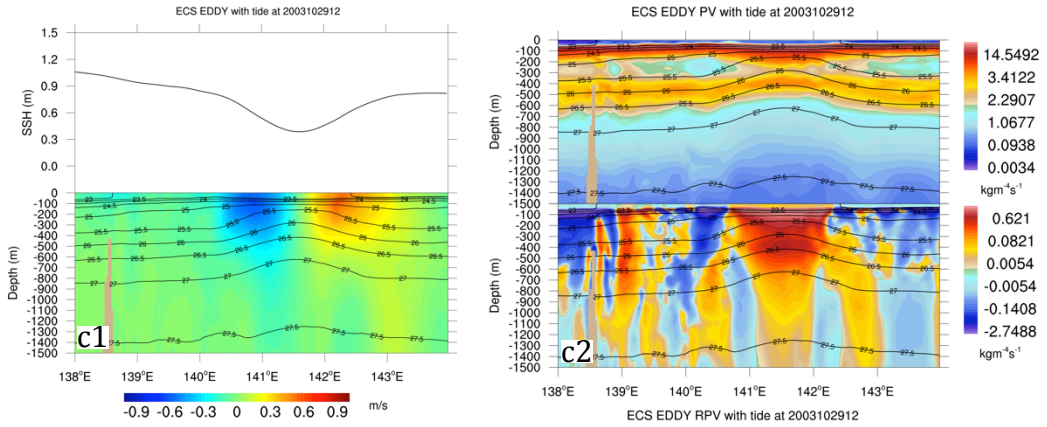
ECS EDDY with tide at 2003102912
ECS EDDY PV with tide at 2003102912
c1
c2
ECS EDDY RPV with tide at 2003102912

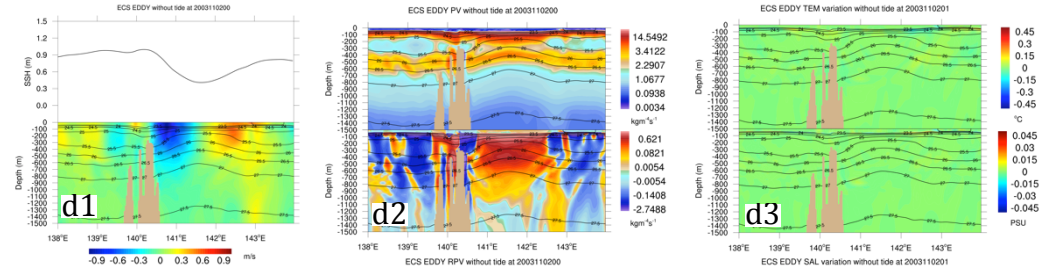
ECS EDDY without tide at 2003110200
ECS EDDY PV without tide at 2003110200
ECS EDDY TEM variation without tide at 2003110201
d1
d2
d3
ECS EDDY RPV without tide at 2003110200
ECS EDDY SAL variation without tide at 2003110201

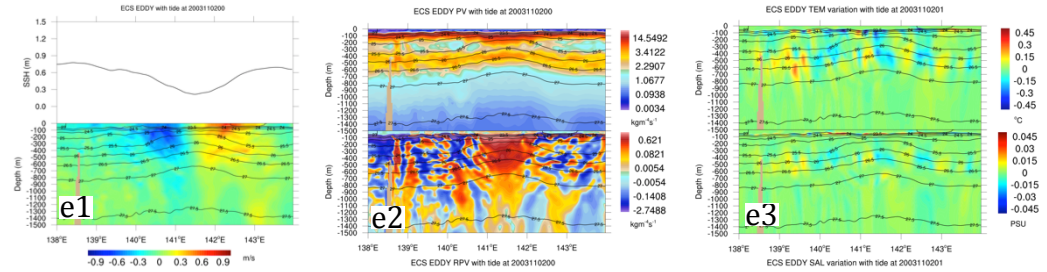
ECS EDDY with tide at 2003110200
ECS EDDY PV with tide at 2003110200
ECS EDDY TEM variation with tide at 2003110201
e1
e2
e3
ECS EDDY RPV with tide at 2003110200
ECS EDDY SAL variation with tide at 2003110201

Fig. 9: Zonal-vertical profile of the eddy
a is plot with C-GLORS weekly average data, the black contour lines in figure is sigma-0 isopycnics; a1 is SSH of eddy (up plot) and normal velocity along zonal section of eddy (down plot) and red shade represent northward velocity, blue shade represent southward velocity; a2 is temperature (up plot) and salinity (down plot) of eddy; a3 is potential vorticity (up plot) and relative potential vorticity (down plot); b is same as a but for ECS-NEMO experiment without tide; c is same as a but for ECS-NEMO with tide experiment; d is same as b but for hourly average data of experiment without tide and d3 is hourly difference of temperature (up plot) and salinity (down plot); e is same as d but for experiment with tide.

5.TIDE SENSITIVITY EXPERIMENT

Most of researches of tide are focus on its effect on shallow sea, such as [12], or deep sea floor, such as [13]. However, eddy can feel sea floor so that tide perhaps can effect eddy in open ocean, especially when eddy close the sea mountain. Thus, we have done two numerical experiments one with tide and another without tide to examine tide's impact on the eddy.

As shown in Fig. 8, the most significant influence of tide is enhancing vertical mix at shallow sea. Tide can bring salt into fresh water near river mouth (Fig. 8a) and upraise cold water of deeper ocean to sea surface (Fig. 8b). By the way, this mixing enhancement is pure dynamic process since we didn't use any tide mixing parameterization scheme in model.

Fig. 9 shows the basic characters of the eddy of C-GLORS. The SSH in the core of this eddy about lower 70 cm than ambient sea and sigma-0 line 25.5 in the core can raised up about 300 m by eddy (Fig. 9a1). Because this is a cyclone eddy, the east part of eddy's current flow to north and west part will flow to south, and the maximum of northward and southward velocity can up to 0.5 m/s. Besides the isopycnics, temperature and salinity also rise up by eddy (Fig. 9a2), so the TS in the surface core of eddy will have some characters of deepen ocean, such as low temperature. Fig. 9a3 is Ertel PV and relative PV; they can reproduce the major structures of eddy clearly. In ambient sea, high PV water appears at the surface and the depth of the upper thermocline, and PV is quite low below the thermocline and between 25 to 25.5 sigma-0 line, relative PV is low everywhere. But at the core of eddy, high PV water can break out low PV belt and conjunct together, and relative PV is rather flat, indicating the nearly solid-body rotation.

The eddy structure of ECS-NEMO experiment without tide similar with C-GLORS and coincide with [14], but slight weaker than latter (Fig. 9b1). The velocity of west part of eddy larger than east part, this notable asymmetry in velocity meaning the eddy movement of model will faster than C-GLORS. Vertical structure of PV and relative PV also similar with C-GLORS, and the high relative PV in west of eddy may be due to the sea mountain in finer bathymetry (Fig. 9b2).

Eddy will even weaker when tide adds in model (Fig. 9c1). The maximum velocity of eddy with tide is the smallest one, and sigma-0 line raise height is the lowest too. There are more high relative PV fragments in ambient water and relative PV at core of eddy relatively narrow in comparison to experiment without tide and C-GLORS (Fig. 9c2). The sigma-0 line 27.5 has some kind of fluctuation in experiment with tide and this more obvious in hourly average plot.

In hourly average analysis (Fig. 9d1, 9d2), eddy almost same with weekly average for experiment without tide. But huge differences will apparent when add tide in model. In Fig.

9e1, eddy looks even weaker than weekly average, and current structure is not flat but in fragments. Although the sigma-0 line 27.5 still has fluctuation, it fluctuates in high frequency and smaller wave rather than low frequency oscillation. Whether the oscillation is tide internal wave or not still need further research. The hourly average has more high relative PV fragments in ambient water than weekly average for experiment with tide (Fig. 9e2). And there are more obvious temperature and salinity time fluctuation for experiment with eddy (Fig. 9e3) than without eddy (Fig. 9d3) in hourly average plot, this indicate there maybe also have some kind of internal wave induced by tide in upper ocean, and this still need further research.

6.CONCLUSION AND FURTHER PLAN

In this research, we implement NEMO in ECS and examine the reproduce ability for tide, Kuroshio and eddy of the new ECS-NEMO by a series numerical sensitivity experiments. We found that the tide simulation is still need improvement in China Sea for z-partial ECS-NEMO. Although the s-sigma model can get much better tide, we still use z-partial edition for further research, because it is easier for nesting z-partial model in a OGCM NEMO such as ORCA-R12 than s-sigma one. We also found that lateral turbulent tracer and momentum diffusion parameterization schemes can affect Kuroshio strength and eddy move path hugely. Bilaplacian can get best simulation in this research and the coefficient less than $6.0 \times 10^8 m^4/s$ is better for reproduce eddy movement. ECS-NEMO can simulate Kuroshio strength even better than reanalysis. However, the Kuroshio water intrusion China Sea has largely differences between bilaplacian coefficients, and this need further compare with observation to make sure which one is best. Beside for shallow sea, tide is also important for eddy since it can produce internal like waves and further impact material exchange between eddy and ambient water.

In future, we plan to apply new bottom boundary friction condition for z-partial NEMO in ECS-NEMO and try to improve its tide simulation ability firstly. And then, we will further research Kuroshio water intrusion China Sea and calculate how many water, salt and energy can enter into China Sea and their climatic influence. Finally, we will examine whether tide produced internal wave can effect eddy or not in open ocean and the extent of tide's impact on material and energy exchange between eddy and ambient water. In addition, tide dynamic for enhance mixing at shallow sea is also one of our further research interesting targets. Thus, two or three articles will in preparing.

Bibliography

[1] Fang Guo-hong. Tides and Tidal Currents in East China Sea, Huanghai Sea and Bohai Sea. In Zhou Di, Liang Yuan-Bo, and Zeng Cheng-Kui, editors, *Oceanology of China Seas SE - 11*, pages 101–112. Springer Netherlands, 1994.

[2] Gurvan Madec. *NEMO ocean engine*. 2012.

[3] S. Andrea and M. Simona. The CMCC Global Ocean Physical Reanalysis System (C-GLORS) version 3.1: Configuration and basic validation. Technical Report December, CMCC, Bologna, 2013.

[4] D. P. Dee, S. M. Uppala, A. J. Simmons, P. Berrisford, P. Poli, S. Kobayashi, U. Andrae, M. A. Balmaseda, G. Balsamo, P. Bauer, P. Bechtold, A. C. M. Beljaars, L. van de Berg, J. Bidlot, N. Bormann, C. Delsol, R. Dragani, M. Fuentes, A. J. Geer, L. Haimberger, S. B. Healy, H. Hersbach, E. V. Hólm, L. Isaksen, P. Kå llberg, M. Köhler, M. Matricardi, A. P. McNally, B. M. Monge-Sanz, J.-J. Morcrette, B.-K. Park, C. Peubey, P. de Rosnay, C. Tavolato, J.-N. Thépaut, and F. Vitart. The ERA-Interim reanalysis: configuration and performance of the data assimilation system. *Quarterly Journal of the Royal Meteorological Society*, 137(656):553–597, April 2011.

[5] Aiguo Dai and Kevin E. Trenberth. Estimates of Freshwater Discharge from Continents: Latitudinal and Seasonal Variations. *Journal of Hydrometeorology*, 3(6):660–687, December 2002.

[6] Aiguo Dai, Taotao Qian, Kevin E. Trenberth, and John D. Milliman. Changes in Continental Freshwater Discharge from 1948 to 2004. *Journal of Climate*, 22(10):2773–2792, May 2009.

[7] M. Zweng, M., R. Reagan, J., I. Antonov, J., A. Locarini, R., V. Mishonov, A., P. Boyer, T., E. Garcia, H., K. Baranova, O., R. Johnson, D., D. Seidov, and M. Biddle, M. WORLD OCEAN ATLAS 2013 Volume 2 : Salinity. In S. Levitus and A. Mishonov, editors, *NOAA Atlas NESDIS 74*, page 39. 2013.

[8] Gary D. Egbert and Svetlana Y. Erofeeva. Efficient Inverse Modeling of Barotropic Ocean Tides. *Journal of Atmospheric and Oceanic Technology*, 19(2):183–204, February 2002.

[9] Changshui Xia, Fangli Qiao, Yongzeng Yang, Jian Ma, and Yeli Yuan. Three-dimensional structure of the summertime circulation in the Yellow Sea from a wave-tide-circulation coupled model. *JOURNAL OF GEOPHYSICAL RESEARCH-OCEANS*, 111(C11):S03, 2006.

[10] G. Shapiro, M. Luneva, J. Pickering, and D. Storkey. The effect of various vertical discretization schemes and horizontal diffusion parameterization on the performance of a 3-D ocean model: the Black Sea case study. *Ocean Science*, 9(2):377–390, March 2013.

[11] M. Andres, M. Wimbush, J.-H. Park, K.-I. Chang, B.-H. Lim, D. R. Watts, H. Ichikawa, and W. J. Teague. Observations of Kuroshio flow variations in the East China Sea. *Journal of Geophysical Research*, 113(C5):C05013, May 2008.

[12] A Guarnieri, N Pinardi, P Oddo, G Bortoluzzi, and M Ravaioli. Impact of tides in a baroclinic circulation model of the Adriatic Sea. *JOURNAL OF GEOPHYSICAL RESEARCH-OCEANS*, 118(1):166–183, 2013.

[13] Harper L. Simmons, Steven R. Jayne, Louis C.St. Laurent, and Andrew J. Weaver. Tidally driven mixing in a numerical model of the ocean general circulation. *Ocean Modelling*, 6(3-4):245–263, January 2004.

[14] H. Nakano, H. Tsujino, and K. Sakamoto. Tracer transport in cold-core rings pinched off from the Kuroshio Extension in an eddy-resolving ocean general circulation model. *Journal of Geophysical Research: Oceans*, 118(10):5461–5488, October 2013.